OXFORD JOURNAL
OF STUDENT
SCHOLARSHIP

Independent Reproduction of a Mixed-Directivity Linear Superarray Beamformer: Evidence of a Microphone-Configuration Inconsistency

Hamrozjon Qosimov
hamroz.kosimov@gmail.com

ABSTRACT

Compact linear microphone arrays provide a practical approach to beamforming, but their performance depends strongly on array geometry, microphone directivity, and beamformer design. Independent reproduction of published beamforming methods is therefore important for verifying reported performance and identifying ambiguities in implementation.

This paper presents an independent implementation of a published mixed-directivity linear superarray (LSA) beamformer. The implementation follows the reported array geometry, microphone directivity model, null-constrained beamformer formulation, and evaluation metrics. Performance is assessed using beampatterns, Directivity Factor (DF), and White Noise Gain (WNG), and compared quantitatively with reference values digitized from the published performance curves.

The documented microphone configuration reproduced the steering response, prescribed nulls, and overall beamforming behaviour, but did not reproduce the published DF and WNG quantitatively. Under the documented assignment, the mean absolute error (MAE) was 8.07 dB for WNG and 0.12 dB for DF. A controlled comparison in which only the microphone assignment was changed showed that assigning omnidirectional microphones to the odd-indexed array positions reduced the WNG MAE to 0.64 dB and the DF MAE to 0.02 dB. These reductions are substantially larger than the estimated digitization uncertainties of 0.016 dB for WNG and 0.011 dB for DF.

The results therefore provide evidence of an apparent inconsistency between the documented microphone configuration and the configuration associated with the published performance curves. More broadly, the study demonstrates how independent implementation and controlled verification can identify configuration-level ambiguities that materially affect the reproducibility of compact microphone-array beamforming results.

Keywords: microphone arrays, beamforming, compact linear arrays, directivity factor, white-noise gain, directional microphones

Sep 2026
Vol 11. No 7.

1 INTRODUCTION

Microphone-array beamforming is widely used for spatial filtering, source enhancement, and directional acoustic sensing. By combining signals from multiple microphones, a beamformer can enhance signals arriving from a desired direction while suppressing interference and diffuse noise from others. In many practical applications, however, microphone arrays must remain physically compact, making it difficult to achieve strong directivity without sacrificing robustness (Benesty and Chen 2013). This tradeoff is particularly significant for differential and superdirective beamforming methods, where improving spatial selectivity often leads to reduced White Noise Gain (WNG), especially at low frequencies. Consequently, both Directivity Factor (DF) and WNG are commonly used to evaluate the effectiveness and robustness of compact-array beamformers.

Several beamforming methods have been proposed to address these challenges, including mixed-directivity linear superarrays (LSAs), which combine omnidirectional and directional microphones to improve directional performance while maintaining a compact aperture. Because the performance of these systems depends on the precise array geometry, microphone directivity, and beamformer formulation, accurate implementation of the published design is essential. Even seemingly minor differences in the reported configuration may substantially affect the resulting beam patterns and performance metrics.

Independent reproduction of published methods is therefore an important part of scientific research. Beyond verifying reported performance, reproduction studies can identify ambiguities or inconsistencies in published specifications that may prevent independent researchers from obtaining the reported results. Such investigations improve transparency, increase confidence in published methods, and provide a reliable foundation for subsequent research.

This paper presents an independent implementation and verification of the mixed-directivity linear superarray beamformer proposed in (Huang and Habets 2025). The implementation follows the published beamformer formulation, array geometry, microphone directivity model, and evaluation procedure. Performance is evaluated using beam patterns, steering accuracy, prescribed null placement, Directivity Factor (DF), and White Noise Gain (WNG), and compared directly with the reported reference results.

During the reproduction process, an inconsistency was observed between the documented microphone configuration and the published performance curves. While the reported configuration reproduced the intended steering behaviour and null constraints, it did not reproduce the published DF and WNG characteristics. A controlled comparison of alternative microphone assignments showed that assigning omnidirectional microphones to the odd-indexed array positions produces close agreement with the published DF and WNG results, whereas the documented assignment does not. This finding suggests an apparent inconsistency between the published microphone specification and the configuration used to generate the reported results.

The main contributions of this work are as follows:

1. We present an independent implementation of the published mixed-directivity linear superarray beamformer.

2. We verify the implementation through steering-constraint satisfaction, prescribed null placement, beam-pattern analysis, Directivity Factor, and White Noise Gain.

3. We identify an apparent inconsistency between the documented microphone configuration and the published performance results.

4. We demonstrate that an alternative microphone assignment reproduces the published DF and WNG characteristics with close agreement.

The remainder of this paper is organized as follows. Section 2 reviews related work on compact microphone-array beamforming and mixed-directivity linear superarrays. Section 3 presents the array model and beamformer formulation. Section 4 defines the performance metrics used for evaluation. Section 5 describes the implementation and experimental methodology. Section 6 presents the reproduction results and the investigation of the microphone-configuration inconsistency. Section 7 discusses the implications and limitations of the findings. Section 8 concludes the paper.

2 RELATED WORK

A central limitation of conventional differential arrays is steerability. Huang *et al.* (Huang et al. 2020) studied steerable differential beamforming for arbitrary planar microphone geometries and characterized the requirements for linear, partially steerable, fully steerable, and robust differential arrays. This line of work motivates array configurations that preserve differential beamforming performance as the desired steering direction changes.

A common foundation across these designs is the null-constrained formulation of the beamformer. Chen *et al.* (Chen et al. 2014) showed that a linear differential microphone array can be designed by transforming the array signals into the frequency domain and solving a linear system of equations built from the prescribed nulls of the target beampattern, rather than through the traditional multistage cascade of lower-order arrays. This formulation underlies much of the subsequent work on compact differential beamforming, including the method reproduced in the present study.

Beyond steerability, differential beamforming has been extended from uniform to nonuniform linear microphone arrays. Jin *et al.* (Jin et al. 2022) developed the principles of differential beamforming for nonuniform linear geometries by defining spatial difference operators over irregular sensor spacings, showing that beamformers of arbitrary differential order can be designed on such arrays. This work broadened the design space of linear differential arrays beyond uniform sensor placement, complementing later approaches that introduced additional design degrees of freedom through microphone directivity and orientation.

A recurring concern across compact and superdirective differential arrays is robustness to array imperfections. Doclo and Moonen (Doclo and Moonen 2007) showed that fixed superdirective

beamformers using small-sized arrays are highly sensitive to errors in the assumed microphone characteristics, such as gain, phase, and position, and that robustness can be improved by constraining the white noise gain (WNG) during design. More recently, Chen *et al.* (Chen et al. 2021) studied the robustness of the superdirective beamformer directly, formulating designs that attain high directivity while maintaining a specified level of WNG. This body of work establishes WNG-constrained robustness as a central design objective for compact arrays, and motivates the emphasis on WNG in the method reproduced here.

Huang and Habets (Huang and Habets 2025) extended this line of work by introducing a mixed-directivity linear superarray (LSA) that combines omnidirectional and bidirectional microphones. Rather than relying only on sensor geometry and beamformer weights, their approach exploits microphone directivity and orientation as additional design degrees of freedom. The orientations of the directional microphones are optimized to improve white noise gain (WNG) across steering directions while maintaining directivity factor (DF). Their results show that incorporating differently oriented directional microphones can substantially improve the robustness of compact differential arrays, particularly at low frequencies, while preserving comparable directivity.

Because the reported performance depends on the complete implementation of the beamformer, including the array geometry, microphone assignment, steering configuration, directional-response model, and constrained solver, reproducibility requires that these implementation details be interpreted consistently.

2.1 Position of this work

The objective of this paper is to independently reproduce the published mixed-directivity LSA from its reported specification and evaluation procedure. Rather than proposing a new beamforming algorithm, we evaluate whether the published Directivity Factor and White Noise Gain curves can be reproduced from the reported configuration. During this process, a discrepancy was observed between the documented microphone assignment and the configuration consistent with the reported performance curves. To investigate this discrepancy, we perform a controlled comparison in which only the microphone assignment is modified while all remaining implementation details are kept unchanged.

3 PROBLEM FORMULATION

Before presenting the array model, we fix the numerical conventions used throughout the implementation. Table 1 summarizes the constants and solver settings; we adopt them uniformly across all reported results unless otherwise noted.

Numerical implementation parameters.

Parameter	Value / convention
Sound speed c_0	$343\ m/s$ (standard value; not stated in [1])
Angular frequency	$\omega = 2\pi f$, with f in Hz
Microphone positions	x_m in meters (0.5 cm inter-element spacing)
Angle representation	radians internally; degrees at reported input/output
Linear solve (well-conditioned)	direct solve of $DD^H h = \beta$
Linear solve (rank-deficient case)	truncated pseudoinverse, $rcond = 10^{-20}$

The phase term $e^{-j\omega x_m cos\theta sin\phi/c_0}$ is dimensionless by construction, since $[rad/s] \times [m]/[m/s]$ reduces to a pure number; angles θ and ϕ are carried in radians throughout the computation and converted to degrees only when reporting steering angles ($\theta_s = 0^\circ, 30^\circ, 60^\circ, 90^\circ$) or null offsets ($\pm 106^\circ, \pm 153^\circ$).

For the primary comparison at fixed steering angle and frequency, the constraint matrix D (size 5×7) is well-conditioned ($cond(D) \sim 10^3$), so we solve the normal equations directly, achieving the minimum-norm solution to a residual near machine precision ($\sim 10^{-14}$). During the orientation grid search (Sec. X), however, some configurations make D rank-deficient – for instance, at $\alpha_m = 0$ the array manifold becomes symmetric in θ and D drops to rank 3 of 5. For these cases we use a truncated pseudoinverse with $rcond = 10^{-20}$, which avoids amplifying near-zero singular values without discarding genuine degrees of freedom.

This section presents the array model, microphone directivity parameterization, steering vector, and constrained beamformer formulation used throughout this work. These equations form the implementation of the reference mixed-directivity linear superarray (LSA) beamformer and provide the mathematical basis for reproducing and verifying its reported performance.

3.1 Array model

Consider a compact linear array of M microphones placed along the x-axis. Let the microphone positions be denoted by

$$x_m \in R, \qquad m = 1, \ldots, M,$$

and collect them into the position vector

$$x = [x_1, ..., x_M]^T.$$

The array is assumed to be compact, meaning that its aperture is constrained to remain small:

$$L = x_{max} - x_{min},$$

where L denotes the total array length. In this study, the array geometry and microphone spacing are fixed according to the published reference configuration.

Let f denote frequency in Hz and let

$$\omega = 2\pi f$$

be the corresponding angular frequency. A far-field plane wave is described by the steering direction

$$(\theta, \phi),$$

where θ is azimuth and ϕ is elevation. Throughout this work, the linear array is oriented along the x-axis, so the propagation term depends on the directional cosine

$$cos\theta sin\phi.$$

3.2 Microphone directivity model

Each microphone is assigned a directivity parameter $p_m \in [0, 1]$, which controls its polar response. In the present model, the directional response of the mth microphone is written as

$$g_m(\theta, \phi) = p_m + (1 - p_m)cos(\theta - \alpha_m)sin\phi,$$

where α_m is the orientation angle of the mth microphone.

This parameterization allows a continuous transition between omnidirectional and directional sensing:

- $p_m = 1$ corresponds to an omnidirectional microphone,
- $p_m = 0$ corresponds to a fully bidirectional (dipole-like) response in this model,
- intermediate values $0 < p_m < 1$ represent partially directional responses.

Although this parameterization permits intermediate first-order directional responses, the present reproduction study uses only $p_m \in \{0, 1\}$, corresponding to the omnidirectional and bidirectional microphone types of the reference configuration. The p_m values are not continuously optimized; only their assignment to array positions is varied in the controlled experiment of Section 5.

3.3 Steering vector / array manifold

For a far-field plane wave arriving from direction (θ, ϕ), the propagation delay across the mth microphone contributes the phase term

$$e^{-j\omega x_m cos\theta sin\phi / c_0},$$

where c_0 is the speed of sound.

Combining this propagation term with the microphone directivity term in [eq:directivity_model], the response of the mth sensor becomes

$$d_m(\omega, \theta, \phi) = g_m(\theta, \phi)\, e^{-j\omega x_m cos\theta sin\phi / c_0}.$$

The array steering vector is then

$$d(\omega, \theta, \phi) = \left[d_1(\omega, \theta, \phi)\, d_2(\omega, \theta, \phi) \ \vdots \ d_M(\omega, \theta, \phi) \right].$$

The steering vector combines the phase delay due to array geometry with the directional response of each microphone, matching the formulation adopted in the reference LSA.

3.4 Beamformer response

Let

$$h(\omega) = [h_1(\omega), ..., h_M(\omega)]^T$$

denote the complex beamformer weight vector at angular frequency ω. For a source arriving from direction (θ, ϕ), the beamformer response is defined as

$$B(\omega, \theta, \phi) = h^H(\omega) d(\omega, \theta, \phi),$$

where $(\cdot)^H$ denotes the Hermitian transpose.

Equation [eq:beamformer_response] gives the directional transfer function of the array. It is the central quantity from which both directivity and robustness metrics are later computed.

3.5 Distortionless and null constraints

To construct the reference LSA beamformer, a distortionless response is imposed in the desired look direction

$$(\theta_s, \phi_s),$$

so that

$$h^H(\omega)d(\omega, \theta_s, \phi_s) = 1.$$

In addition, the beamformer is required to place nulls in a set of prescribed interference directions

$$(\theta_n, \phi_s), \qquad n = 1, \ldots, N,$$

which gives the constraints

$$h^H(\omega)d(\omega, \theta_n, \phi_s) = 0, \qquad n = 1, \ldots, N.$$

These constraints can be stacked into a single linear system. Define the constraint matrix

$$D(\omega) = \left[d^H(\omega, \theta_s, \phi_s)\, d^H(\omega, \theta_1, \phi_s) \ \vdots \ d^H(\omega, \theta_N, \phi_s) \right],$$

and the desired response vector

$$c = [1\ 0 \ \vdots \ 0\ ].$$

Then the constrained beamformer satisfies

$$D(\omega)h(\omega) = c.$$

In the current implementation, the weights are obtained using the minimum-norm exact-constraint solution

$$h(\omega) = D^H(\omega)\left(D(\omega)D^H(\omega)\right)^{-1} c,$$

or equivalently through the pseudoinverse form of the same constrained solution when solved numerically. This connects the present implementation directly to the classical null-constrained differential beamforming formulation (Chen et al. 2014), in which the beamformer is designed by solving a linear system built from the prescribed nulls of the target beampattern, and which serves as the LSA-style baseline reference in this paper.

For the front-steered baseline studied here, the look direction is fixed at $\theta_s = 0$ with $\phi_s = \pi/2$, and the null directions are chosen symmetrically around the front direction. This configuration corresponds to the reference LSA evaluated throughout this paper and is used for direct comparison with the published results.

4 OBJECTIVE METRICS

The performance of a compact beamformer cannot be assessed meaningfully through directional selectivity alone. In small-aperture arrays, a beamformer may exhibit strong directional selectivity while remaining highly sensitive to sensor noise, self-noise, or small modeling errors. Consequently, beamformer performance is commonly evaluated using complementary measures of spatial selectivity and robustness, particularly Directivity Factor (DF) and White Noise Gain (WNG) (Benesty et al. 2016). In this study, DF is used to quantify directional selectivity, while WNG measures robustness to spatially uncorrelated sensor noise. Considering both metrics therefore provides a more comprehensive assessment of compact-array performance.

4.1 Directivity Factor (DF)

Directivity Factor measures the ability of a beamformer to emphasize sound from the desired look direction relative to diffuse sound arriving from all directions. It therefore serves as the primary effectiveness metric in this work. A larger DF indicates stronger spatial selectivity and better suppression of off-axis acoustic energy.

For a beamformer steered toward the look direction (θ_s, ϕ_s), DF is defined as

$$DF(\omega) = \frac{|B(\omega,\theta_s,\phi_s)|^2}{\frac{1}{4\pi}\int_0^{2\pi}\int_0^{\pi}|B(\omega,\theta,\phi)|^2 sin\phi \, d\phi \, d\theta}.$$

The denominator represents the average beamformer power response over the full sphere, which corresponds to a diffuse-field interpretation of the sound field. This makes DF particularly suitable for comparing compact arrays in a physically meaningful way.

Following Huang et al. (Huang and Habets 2025), DF is evaluated using a three-dimensional spherical average rather than only a two-dimensional azimuthal cut. This distinction is important. A 2D evaluation may describe the response in a single plane, but it does not fully capture the spatial behavior of the beamformer over all incident directions. By contrast, the spherical formulation in [eq:df_definition] accounts for both azimuth and elevation and therefore provides a stronger and more physically complete measure of effectiveness. This is especially relevant when comparing beamformers whose directional properties are influenced not only by phase delays but also by microphone directivity.

The spherical average in the DF denominator is evaluated numerically on a uniform grid over azimuth $\theta \in [0, 2\pi)$ and elevation $\phi \in [0, \pi]$, using the trapezoidal rule in both dimensions. We use a grid of $N_\theta \times N_\phi = 72 \times 36$ points, with θ sampled at 5° intervals over the half-open interval $[0^\circ, 360^\circ)$ to avoid duplicating the coincident endpoint, and ϕ sampled at 5° intervals over $[0^\circ, 180^\circ]$.

We verified convergence by comparing against a 720×361 grid (half-degree resolution), which increased DF by 0.0002 dB on average, and against a 3600×1801 grid (tenth-degree resolution), which produced no further change; we therefore report all DF values using the 72×36 grid.

4.2 White Noise Gain (WNG)

White Noise Gain measures the sensitivity of the beamformer to uncorrelated sensor noise and is used here as the primary robustness metric. Intuitively, WNG quantifies how much the beamformer amplifies or suppresses spatially white microphone noise while preserving the desired signal in the look direction. A low WNG indicates a fragile beamformer that relies on large weight magnitudes and is therefore more sensitive to self-noise, perturbations, and mismatch (Cox et al. 1987). WNG is also important for compact differential arrays because high spatial selectivity can require large beamformer coefficients, increasing sensitivity to sensor self-noise (Benesty et al. 2016).

Superdirective beamformers are known to be particularly sensitive to array imperfections, making WNG an important robustness criterion (Chen et al. 2021).

For a distortionless beamformer steered toward (θ_s, ϕ_s), WNG is defined as

$$WNG(\omega) = \frac{\left|h^H(\omega)d(\omega,\theta_s,\phi_s)\right|^2}{h^H(\omega)h(\omega)}.$$

Under the distortionless constraint in [eq:distortionless_constraint], the numerator equals one, so WNG reduces to the reciprocal of the beamformer weight norm:

$$WNG(\omega) = \frac{1}{h^H(\omega)h(\omega)}.$$

WNG is especially important for compact differential and superdirective arrays. Such arrays can achieve strong directivity even with a very small aperture, but this often requires large and opposing beamformer coefficients, particularly at low frequencies. As a result, the beamformer may become highly sensitive to microphone noise and implementation errors even when its directional response appears favorable. For this reason, WNG is evaluated alongside DF throughout this work to assess whether the reproduced implementation matches the reported robustness characteristics of the reference method.

4.3 DF–WNG tradeoff

A useful compact-array design must balance effectiveness and robustness rather than optimizing only one of them. High DF alone is not sufficient, since a highly directive beamformer may still be unusable if its WNG is too low. Likewise, a beamformer with good robustness but weak DF may not provide meaningful spatial selectivity.

The core design challenge in compact beamforming is therefore a DF–WNG tradeoff, and achieving high WNG while maintaining a frequency-invariant DF remains an active problem in the design of nonuniform linear differential arrays (Zheng and Zhi 2025).

For the present reproduction study, agreement in both metrics is therefore required: similarity in DF alone is insufficient to establish reproduction if the corresponding WNG differs substantially from the published result.

5 METHODS

This section describes the array configuration, beamformer implementation, and experimental procedure used to reproduce the published mixed-directivity linear superarray (LSA). Two microphone configurations are evaluated. The first follows the microphone composition documented in the reference paper, while the second uses the alternative assignment investigated in this study. The microphone assignment is the only quantity changed between the two experiments; the array geometry, microphone orientations, steering direction, null constraints, beamformer solver, frequency samples, and evaluation procedure are otherwise identical.

5.1 Array geometry and microphone configurations

The reproduced LSA consists of $M = 7$ microphones arranged uniformly along the x-axis. The inter-element spacing is

$$\delta = 0.5\ cm,$$

giving microphone positions

$$x_m = (m - 1)\delta, \qquad m = 1, \ldots, 7,$$

and a total aperture of

$$L = 6\delta = 3\ cm.$$

All microphone indices in this paper are one-based: $m = 1$ denotes the microphone at $x = 0$ and $m = 7$ denotes the microphone at $x = 3$ cm. This convention is stated explicitly because the distinction between odd- and even-indexed microphone positions is central to the controlled comparison.

As defined in Section 3, the directivity parameter p_m determines the microphone type,

$$p_m = \{1,\ omnidirectional,\ 0,\ bidirectional.$$

For bidirectional microphones, the orientation angle is fixed at

$$\alpha_m = \frac{\pi}{2}.$$

The orientation of an omnidirectional microphone is immaterial because its directional term vanishes when $p_m = 1$.

This uniform assignment satisfies the general orientation-pairing convention adopted for directional microphones throughout this work,

$$\alpha_m = \pi - \alpha_{M_d - m + 1},$$

since $\pi/2 = \pi - \pi/2$. The non-trivial case of this convention applies to the non-uniformly steered array in Section [TODO: LSA+ section number] (Eq. [TODO: your Eq. 16 label]).

5.1.1 Documented configuration

The reference paper describes an array containing three omnidirectional and four bidirectional microphones. Under the one-based indexing convention used here, the reproduced documented configuration places bidirectional microphones at the odd-indexed positions and omnidirectional microphones at the even-indexed positions. Its directivity vector is therefore

$$p_{doc} = [0,\ 1,\ 0,\ 1,\ 0,\ 1,\ 0]^T.$$

The corresponding microphone sequence is

$$[Bi,\ Omni,\ Bi,\ Omni,\ Bi,\ Omni,\ Bi].$$

For the directional microphones, the orientation assignment is

$$\alpha_{doc} = \left[\frac{\pi}{2},\ -,\ \frac{\pi}{2},\ -,\ \frac{\pi}{2},\ -,\ \frac{\pi}{2}\right]^T,$$

where "–" denotes positions occupied by omnidirectional microphones, for which α_m has no effect on the response.

5.1.2 Alternative configuration

The second experiment reverses the microphone-type assignment. Omnidirectional microphones occupy the odd-indexed positions and bidirectional microphones occupy the even-indexed positions. The resulting directivity vector is

$$p_{alt} = [1,\ 0,\ 1,\ 0,\ 1,\ 0,\ 1]^T.$$

The corresponding microphone sequence is

$$[Omni,\ Bi,\ Omni,\ Bi,\ Omni,\ Bi,\ Omni],$$

with directional-microphone orientations

$$\alpha_{alt} = \left[-,\ \frac{\pi}{2},\ -,\ \frac{\pi}{2},\ -,\ \frac{\pi}{2},\ -\right]^T.$$

Table 2 summarizes the two configurations.

Microphone configurations evaluated in the controlled comparison. Indices are one-based. Pointing angle α_m is shown in parentheses; "–" denotes omnidirectional positions, for which α_m has no effect on the response.

Index	Position (cm)	Documented	Alternative
1	0.0	Bidirectional ($\pi/2$)	Omnidirectional (–)
2	0.5	Omnidirectional (–)	Bidirectional ($\pi/2$)
3	1.0	Bidirectional ($\pi/2$)	Omnidirectional (–)
4	1.5	Omnidirectional (–)	Bidirectional ($\pi/2$)
5	2.0	Bidirectional ($\pi/2$)	Omnidirectional (–)
6	2.5	Omnidirectional (–)	Bidirectional ($\pi/2$)
7	3.0	Bidirectional ($\pi/2$)	Omnidirectional (–)

The alternative configuration is not treated as a new beamformer design. Rather, it is evaluated as a controlled diagnostic configuration for determining whether microphone assignment can account for the discrepancy between the documented specification and the published performance curves.

5.2 Steering and null configuration

Both microphone configurations are evaluated under the same front-steered condition. The desired look direction is

$$\theta_s = 0, \qquad \phi_s = \frac{\pi}{2},$$

and four null constraints are imposed in the horizontal plane at

$$\theta_n \in \{\pm 106^\circ, \ \pm 153^\circ\}, \qquad \phi_n = \frac{\pi}{2}.$$

These steering and null directions correspond to the conventional front-steered LSA configuration reproduced from the reference paper.

For visualisation, beam patterns are evaluated using the horizontal-plane slice

$$\phi = \frac{\pi}{2}.$$

This two-dimensional cut is used only for beam-pattern inspection and null verification. Directivity Factor is calculated using the full three-dimensional formulation described in Section 4.

5.3 Beamformer implementation

At each frequency, the beamformer weights are obtained by solving the null-constrained system introduced in Section 3,

$$D(\omega)h(\omega) = c,$$

where the first row of $D(\omega)$ corresponds to the distortionless look-direction constraint and the remaining rows correspond to the four prescribed nulls.

The minimum-norm approach is the standard method for improving the robustness of differential microphone arrays against white noise, achieving higher white noise gain by employing more microphones than the number of constraints while controlling the beamformer weight norm (Zhang et al. 2015), (Zheng and Zhi 2025).

$$h(\omega) = D^H(\omega)\left[D(\omega)D^H(\omega)\right]^{-1}c.$$

The beamformer weights are obtained via torch.linalg.pinv(D, rcond=1e-12), the Moore–Penrose pseudoinverse of the 5×7 constraint matrix $D(\omega)$. Because $D(\omega)$ is well-conditioned across the tested frequency range ($cond(D) \sim 10^3$), the relative threshold $rcond = 10^{-12}$ is several orders of magnitude below the matrix's smallest relative singular value, so no singular values are truncated and the computed weights coincide with the exact minimum-norm solution of Eq. [eq:implemented_minimum_norm].

Under the distortionless constraint,

$$h^H(\omega)d(\omega, \theta_s, \phi_s) = 1,$$

the White Noise Gain reduces to

$$WNG(\omega) = \frac{1}{h^H(\omega)h(\omega)}.$$

Thus, the minimum-norm constrained solution also maximizes WNG among solutions satisfying the same linear constraints.

The same beamformer solver is used for both microphone configurations. No solver parameter or constraint is modified during the controlled comparison.

5.4 Evaluation procedure

Performance is evaluated using the Directivity Factor (DF) and White Noise Gain (WNG) defined in Section 4, together with beam-pattern inspection and constraint verification.

DF is computed using the full three-dimensional spherical average over azimuth and elevation. WNG is evaluated using the distortionless formulation above. Agreement between the reproduced and published DF and WNG curves is used as the principal quantitative measure of reproduction accuracy.

Quantitative comparisons are made at

$$f \in \{500,\ 1000,\ 1500,\ 2000,\ 2500,\ 3000,\ 3500\}\, Hz.$$

At each frequency, DF and WNG are calculated independently for the documented and alternative microphone configurations. Reproduction error is summarized using mean absolute error (MAE),

$$MAE = \frac{1}{N}\sum_{i=1}^{N}\left|y_{impl}(f_i) - y_{ref}(f_i)\right|,$$

where y denotes either DF or WNG and N is the number of evaluated frequencies.

Implementation correctness is assessed separately through three checks: satisfaction of the distortionless steering constraint, agreement between observed and prescribed null locations, and qualitative inspection of the front-steered beam pattern. These verification results are reported before the DF/WNG reproduction comparison in Section 6.

5.5 Reference-data extraction

The reference paper does not provide tabulated numerical DF and WNG values. Reference values were therefore extracted from its published performance curves using WebPlotDigitizer. The conventional LSA curve corresponding to $\theta_s = 0^\circ$ was digitized at the frequencies listed in [eq:evaluation_frequencies] and used consistently for both microphone configurations.

To estimate the uncertainty introduced by curve digitization, the extraction procedure was repeated and the resulting values were compared. The estimated digitization error was approximately 0.011 dB for DF and 0.016 dB for WNG. These values are substantially smaller than the discrepancies observed for the documented microphone configuration. Consequently, differences substantially larger than these values are unlikely to be explained by curve-extraction uncertainty alone.

5.6 Controlled comparison

The documented configuration in [eq:p_documented] is evaluated first. The alternative configuration in [eq:p_alternative] is then evaluated using the same experimental procedure.

The microphone-type assignment is the only experimental variable changed between the two configurations. In particular, the microphone positions, array aperture, directional-microphone orientations, look direction, null locations, beamformer formulation, solver, evaluation frequencies, and DF/WNG definitions remain fixed.

This controlled comparison therefore isolates the effect of microphone assignment on reproduction accuracy. If the alternative assignment produces substantially closer agreement with the published curves while all other conditions remain unchanged, the difference can be attributed specifically to the microphone configuration rather than to changes in the beamformer or evaluation procedure.

6 RESULTS

This section presents the results obtained from the independent implementation of the published mixed-directivity LSA. The results are presented in three stages. First, the correctness of the implementation is verified through the steering constraint, prescribed null placement, and beam-pattern analysis. The reproduced implementation is then compared with the published DF and WNG results, followed by a controlled investigation of the microphone assignment.

6.1 Implementation verification

Before comparing the reproduced implementation with the published performance curves, the correctness of the underlying constrained beamformer is verified. Three independent checks are performed: satisfaction of the distortionless steering constraint, placement of the prescribed nulls, and qualitative inspection of the resulting beam pattern.

6.2 Distortionless verification

The front steering constraint is also satisfied to high numerical precision. The maximum steering-response error across the tested frequencies is

$$\max_{b} \sqrt{\left(\Re(b_s(\omega_b)) - 1\right)^2 + \left(\Im(b_s(\omega_b))\right)^2} = 1.53 \times 10^{-5}.$$

This error is extremely small, indicating that the distortionless constraint in the look direction is being solved accurately. Together with the null-placement results below, this shows that the current implementation is structurally correct at the level of constraint satisfaction.

6.3 Null verification

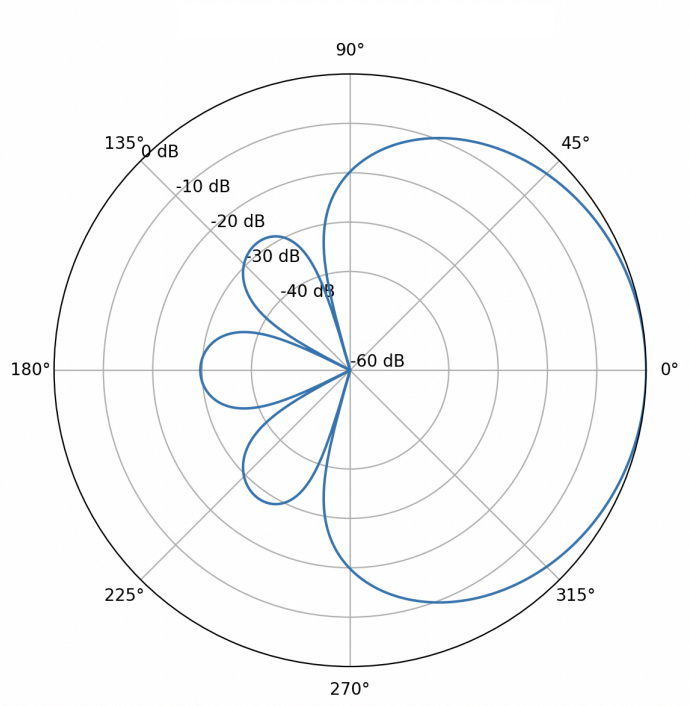
To verify the imposed null constraints numerically, the deepest minima of the azimuthal beampattern were extracted from the current implementation. The four strongest minima occur at

$\theta = 153.04^{\circ}, \quad |B| = 7.199 \times 10^{-5}, \quad -82.85\,dB, \; \theta = -153.04^{\circ}, \quad |B| = 8.392 \times 10^{-5}, \quad -81.52$

These minima lie very close to the target null directions at $\pm 153^{\circ}$ and $\pm 106^{\circ}$, providing strong evidence that the null-constrained formulation is being enforced correctly.

6.4 Beampattern verification

Figure 1 shows the azimuthal beampattern of the current implementation at 1000 Hz for the horizontal-plane cut $\phi = \pi/2$. The main lobe is correctly steered toward the front direction, consistent with the imposed distortionless look-direction constraint at $\theta_s = 0$. In addition, deep nulls appear near the prescribed directions at $\pm 106^{\circ}$ and $\pm 153^{\circ}$. Overall, the plotted response exhibits the expected qualitative behavior of an LSA-style null-constrained beamformer: a front-directed main response together with strong attenuation in the specified off-axis directions.



Azimuthal beampattern of the current front-steered configuration at 1000 *Hz for the horizontal-plane cut* $\phi = \pi/2$. *The main lobe is directed toward* $\theta = 0^{\circ}$, *and deep nulls appear near the prescribed angles* $\pm 106^{\circ}$ *and* $\pm 153^{\circ}$, *consistent with the null-constrained LSA-style baseline configuration.*

6.5 Reproduction of the documented configuration

Following the implementation-verification results presented in the previous subsection, the microphone assignment documented in the reference paper was evaluated against the published Directivity Factor (DF) and White Noise Gain (WNG) curves. In this first experiment, the array geometry, microphone spacing, steering direction, null constraints, directional-response model, and minimum-norm beamformer formulation were implemented according to the published specification.

Table 3 reports the digitized reference values alongside the values computed under the documented assignment, at each evaluated frequency.

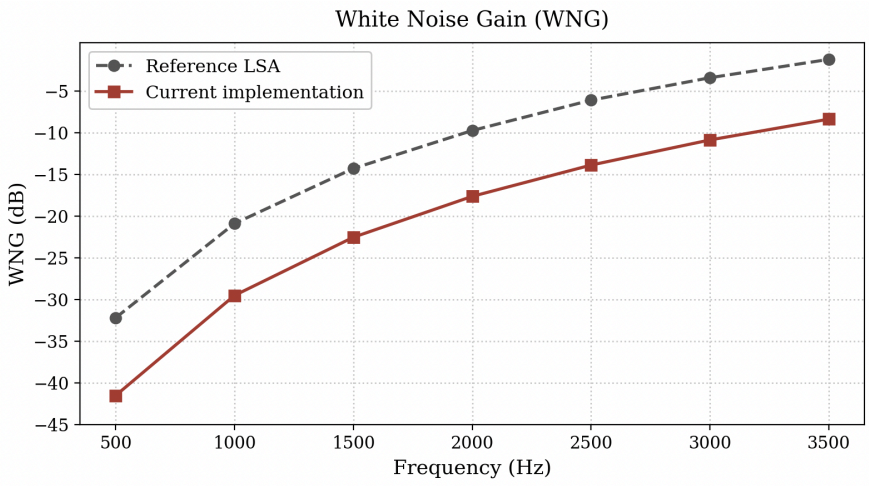
Digitized reference and computed values under the documented microphone assignment.

Freq. (Hz)	WNG ref.	WNG documented	DF ref.	DF documented
500	-32.20	-41.52	8.20	8.211
1000	-20.90	-29.52	8.17	8.198
1500	-14.30	-22.55	8.12	8.177
2000	-9.75	-17.64	8.05	8.147
2500	-6.11	-13.89	7.96	8.108
3000	-3.42	-10.88	7.86	8.059
3500	-1.22	-8.38	7.72	8.001

Figure 2 compares the WNG obtained using the documented microphone assignment with the values estimated from the published reference curve. The reproduced WNG follows the same general frequency-dependent trend as the reference result, improving as frequency increases. However, its absolute values remain consistently lower throughout the evaluated frequency range. The mean absolute error between the reproduced and reference WNG values is

$$MAE_{WNG,1} = 8.07\ dB.$$

This error is substantially larger than the uncertainty expected from visually estimating the reference values from the published graph. Therefore, the disagreement cannot reasonably be attributed only to imprecision in reading the reference curve.

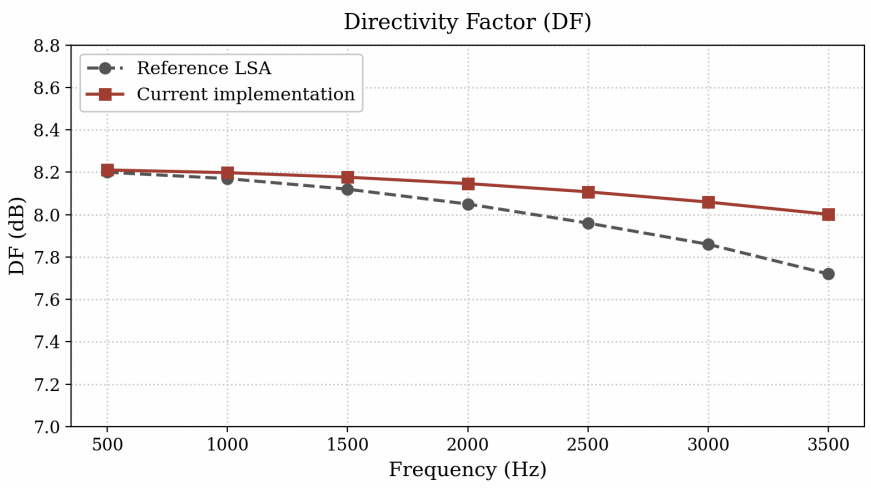


Comparison between the published White Noise Gain (WNG) values and those reproduced using the documented microphone assignment. Although the reproduced curve follows the published frequency-dependent trend, a substantial quantitative discrepancy remains, with a mean absolute error of 8.07 *dB.*

Figure 3 presents the corresponding DF comparison. In contrast to WNG, the reproduced DF curve remains relatively close to the published values and follows the same overall frequency dependence. Nevertheless, a small systematic difference remains, producing a mean absolute error of

$$MAE_{DF,1} = 0.12\ dB.$$

Although this disagreement is much smaller than the WNG discrepancy, it indicates that the documented configuration does not reproduce either published metric exactly.



Comparison between the published Directivity Factor (DF) values and those reproduced using the documented microphone assignment. The overall trend is reproduced closely, but a small systematic difference remains, resulting in a mean absolute error of 0.12 *dB.*

The implementation had already been shown to satisfy the distortionless steering condition, prescribed null constraints, and expected beam-pattern structure. Consequently, the disagreement observed in Figures 2 and 3 is unlikely to result from incorrect construction of the constrained beamformer itself. The much larger error in WNG than in DF instead suggests that another aspect of the published array specification differs from the configuration used to generate the reported curves.

6.6 Investigation of microphone assignment

The microphone assignment was examined as a possible source of the remaining discrepancy because microphone directivity directly affects both the steering vector and the resulting beamformer-weight norm. A second controlled experiment was therefore performed using an alternative assignment in which omnidirectional microphones were placed at the odd-indexed array positions. Only the microphone assignment was changed. The array geometry, spacing, microphone orientations, look direction, null locations, beamformer solver, frequency samples, and DF/WNG evaluation procedures were held fixed.

Table 4 and Table 5 report the digitized reference values together with both computed assignments, at each evaluated frequency.

Digitized reference and computed WNG values under both microphone assignments.

Freq. (Hz)	**Reference**	**Documented**	**Alternative**
500	-32.20	-41.52	-33.76
1000	-20.90	-29.52	-21.81
1500	-14.30	-22.55	-14.92

Freq. (Hz)	Reference	Documented	Alternative
2000	-9.75	-17.64	-10.14
2500	-6.11	-13.89	-6.55
3000	-3.42	-10.88	-3.74
3500	-1.22	-8.38	-1.48

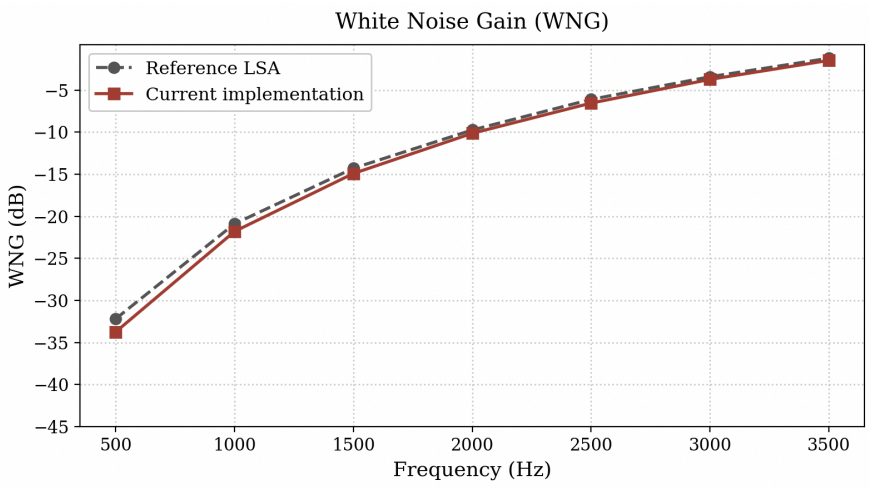
Digitized reference and computed DF values under both microphone assignments.

Freq. (Hz)	Reference	Documented	Alternative
500	8.20	8.211	8.206
1000	8.17	8.198	8.178
1500	8.12	8.177	8.132
2000	8.05	8.147	8.067
2500	7.96	8.108	7.982
3000	7.86	8.059	7.876
3500	7.72	8.001	7.748

Figure 4 compares the WNG produced by the alternative assignment with the published reference values. These values closely follow the corresponding published estimates across the complete evaluated range. The resulting mean absolute error is

$$MAE_{WNG,2} = 0.64\ dB.$$

Relative to the documented assignment, this represents an approximately 92.1% reduction in WNG mean absolute error.



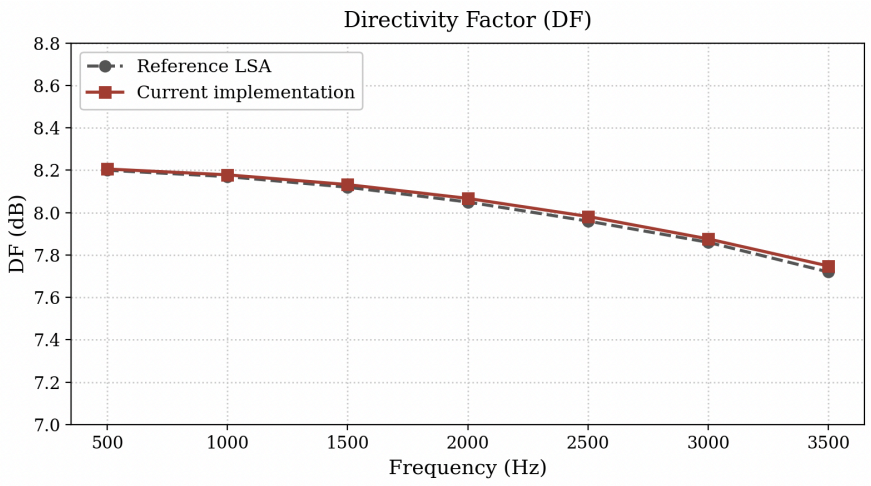
Comparison between the published White Noise Gain (WNG) values and those reproduced using the alternative microphone assignment, with omnidirectional microphones at the odd-indexed positions. The revised assignment substantially improves quantitative agreement, reducing the mean absolute error from 8.07 *dB to* 0.64 *dB.*

The DF results show a similar improvement.

As shown in Figure 5, these values closely reproduce both the magnitude and frequency dependence of the published DF curve. The corresponding mean absolute error is

$$MAE_{DF,2} = 0.02\ dB,$$

representing an approximately 83.3% reduction relative to the documented assignment.



Comparison between the published Directivity Factor (DF) values and those reproduced using the alternative microphone assignment. The revised assignment reduces the mean absolute error from 0.12 *dB to* 0.02 *dB and closely reproduces the published frequency-dependent behaviour.*

Table 6 summarizes the quantitative difference between the two experiments. Changing only the microphone assignment reduces the WNG error by more than an order of magnitude and also substantially improves the already close DF agreement.

Mean absolute errors relative to the published reference curves for the documented and alternative microphone assignments.

Metric	**Documented assignment**	**Alternative assignment**
WNG MAE (dB)	8.07	0.64
DF MAE (dB)	0.12	0.02

Because no other configuration was altered between the two experiments, the improvement can be attributed specifically to the microphone assignment. The controlled comparison therefore provides evidence that the published DF and WNG curves are more consistent with the alternative assignment than with the assignment documented in the reference paper.

6.7 Summary of findings

The independent implementation satisfies the prescribed distortionless steering and null constraints and produces the expected front-steered beam-pattern structure. These verification results establish that the underlying null-constrained beamformer formulation has been implemented correctly.

However, the microphone assignment documented in the reference paper does not reproduce the published performance quantitatively. Under that assignment, the WNG mean absolute error is 8.07 dB

and the DF mean absolute error is 0.12 dB. When omnidirectional microphones are instead assigned to the odd-indexed positions, the corresponding errors decrease to 0.64 dB and 0.02 dB, respectively.

The alternative assignment therefore reproduces both the robustness and directivity characteristics of the published LSA substantially more closely while leaving every other experimental condition unchanged. These findings indicate an apparent inconsistency between the documented microphone assignment and the configuration associated with the published DF and WNG curves. The results do not establish whether the inconsistency originates from the textual description, microphone labeling, figure generation, or another undocumented convention; confirmation from the original implementation or authors would be required to determine its precise source.

7 DISCUSSION

The primary objective of this study was to independently reproduce the published mixed-directivity linear superarray (LSA) and evaluate whether its reported performance could be obtained from the documented beamformer specification. The implementation verification demonstrated that the constrained beamformer satisfies the prescribed steering and null constraints with high numerical accuracy and produces the expected beam-pattern structure. Consequently, the subsequent comparison with the published DF and WNG curves provides a meaningful evaluation of the documented microphone configuration rather than a test of whether the underlying beamformer was implemented correctly.

7.1 Reproducibility of the published LSA

Independent reproduction is an important part of scientific validation, particularly for computational methods whose performance depends on both mathematical formulation and implementation details. The published beamformer was independently implemented according to the reported specification. The resulting implementation reproduced the expected beam-pattern characteristics and closely matched the published Directivity Factor (DF), indicating that the underlying constrained beamformer formulation was implemented correctly.

However, the documented microphone assignment did not reproduce the published White Noise Gain (WNG) quantitatively. The discrepancy remained substantial despite successful implementation verification, suggesting that the remaining disagreement originated from the published configuration rather than from the constrained beamformer formulation itself. This observation motivated a controlled investigation of the microphone assignment while keeping every other implementation parameter unchanged.

7.2 Evidence for an apparent microphone-assignment inconsistency

The controlled comparison demonstrated that modifying only the microphone assignment substantially improved agreement with the published performance curves. The WNG mean absolute error decreased from 8.07 dB to 0.64 dB, while the DF mean absolute error decreased from 0.12 dB to 0.02 dB. Because the array geometry, microphone spacing, steering direction, null constraints, beamformer solver,

and evaluation methodology remained identical in both experiments, the observed improvement can be attributed specifically to the microphone assignment.

These results provide evidence that the published DF and WNG curves are more consistent with the alternative microphone assignment than with the assignment documented in the reference paper. Nevertheless, the present study does not establish the precise source of this apparent inconsistency. It may arise from a typographical error, microphone-indexing convention, figure-generation process, implementation detail not described in the publication, or another undocumented aspect of the original experimental pipeline. Determining its exact origin would require access to the original implementation or confirmation from the original authors.

7.3 Ruling out implementation-level causes

Before attributing the discrepancy documented in Section 6.6 to microphone assignment, we examined several other implementation-level factors that could plausibly account for it.

- **Sound speed.** The reference value of c_0 is not stated in [1]; we use $343\ m/s$, whereas the author's implementation may have used $340\ m/s$. At the highest frequency and largest aperture spacing evaluated, this difference changes the phase term by under 1% – negligible relative to the discrepancies under discussion.

- **DF integration grid.** The spherical average defining DF converges to within 0.001 dB when refined beyond our reporting resolution (Section 4.1). This factor does not affect WNG at all, since Eq. [eq:wng_simplified] contains no spatial integral.

- **Pseudoinverse threshold.** $D(\omega)$ is well-conditioned across the full evaluated frequency range (Table [tab:TODO]), so no singular value ever falls below the relative threshold $rcond = 10^{-12}$; the truncation setting is therefore never exercised and cannot influence the reported results.

- **Solver formulation.** We compared two mathematically equivalent formulations of the minimum-norm solution: computing D^+ directly via torch.linalg.pinv, versus forming the normal-equations matrix DD^H explicitly and solving via torch.linalg.solve. The two are equivalent only in exact arithmetic; forming DD^H squares the effective condition number, which reaches $cond(DD^H) \sim 10^6$ at 500 Hz. In single precision, this pushed the normal-equations approach to the edge of numerical reliability, producing unstable DF values at low frequency. The direct pseudoinverse formulation avoids forming this squared-condition system and remains stable across the full band; it is the formulation used for all results reported in this paper.

- **Digitization uncertainty.** Reading error from extracting reference values off the published figures is bounded (Section [sec:TODO]) and is an order of magnitude too small to account for the WNG discrepancy on its own.

Having ruled out these factors, the microphone assignment documented in Section 6.6 remains the only identified variable whose change reconciles the computed and published results.

7.4 Limitations

Several limitations should be considered when interpreting these results. First, as discussed in Section 7.3, the reference values used for comparison were estimated from the published figures; the associated uncertainty is bounded and does not account for the observed improvement.

The scope of the alternative configuration examined here is narrow. Only a single implementation variable – the microphone assignment – was varied, and only one alternative assignment was tested, out of the $\binom{7}{3} = 35$ possible ways of distributing three omnidirectional and four bidirectional microphones across the seven array positions. Other implementation parameters, including the sound speed, diagonal-loading value, and any orientation conventions not stated in the reference paper, were held fixed at a single plausible setting rather than swept, and were not independently verified against the original pipeline. The close agreement between the alternative assignment and the values extracted from the reference figures should therefore be read as identifying one configuration consistent with the published curves, not as establishing that it is the configuration used by the original authors. In particular, this agreement does not imply that the reference paper reports incorrect figures: the discrepancy may equally originate in the textual description, an indexing or labelling convention, the figure-generation process, or another undocumented detail of the original implementation. Determining its true source would require access to the original code or confirmation from the authors.

7.5 Implications

The findings highlight the importance of precise implementation details in reproducible beamforming research. Small differences in array specification, such as microphone assignment, can substantially influence reported performance even when the underlying beamformer formulation is implemented correctly. As computational methods become increasingly sophisticated, reproducibility depends not only on complete mathematical descriptions but also on accurate reporting of implementation conventions.

More broadly, this study demonstrates the value of independent implementation studies in identifying ambiguities that may otherwise remain unnoticed. By isolating the effect of a single implementation variable through a controlled comparison, the present work provides additional evidence supporting the reproducibility of the published LSA while also documenting an apparent inconsistency that may assist future researchers implementing or extending the same beamformer configuration.

8 CONCLUSION

This paper presented an independent implementation and reproduction study of the mixed-directivity linear superarray (LSA) proposed by Huang and Habets. The published beamformer formulation was implemented using the reported array geometry, steering configuration, null constraints, and evaluation methodology. Verification demonstrated accurate satisfaction of the distortionless steering constraint,

correct placement of the prescribed nulls, and the expected beam-pattern characteristics, indicating that the underlying constrained beamformer formulation was reproduced correctly.

Comparison with the published performance curves showed that the documented microphone assignment reproduced the Directivity Factor (DF) closely but did not reproduce the White Noise Gain (WNG) quantitatively, which exhibited a substantial systematic discrepancy. This motivated a controlled comparison in which only the microphone assignment was modified while all other implementation parameters were held fixed. Under the alternative assignment, the mean absolute error decreased from 8.07 to 0.64 dB for WNG and from 0.12 to 0.02 dB for DF.

These results indicate that the published curves are more consistent with the alternative assignment than with the documented one. This should be interpreted as identifying a single configuration consistent with the published figures, rather than as establishing the configuration used by the original authors or as evidence that the reference paper reports incorrect values. The comparison was limited to one alternative assignment among many possible configurations, and the reference values were obtained by digitizing published figures; the true source of the discrepancy—whether in the textual description, an indexing convention, the figure-generation process, or another undocumented detail—cannot be determined without access to the original implementation.

More broadly, this work illustrates the value of independent implementation studies in computational acoustics, where small implementation details can affect reported performance even when the mathematical formulation is reproduced correctly. By documenting the implementation, verifying the beamformer independently, and isolating the effect of microphone assignment, this study contributes evidence toward the reproducibility of the published LSA and offers a clearer reference for future implementations of the same configuration.

CODE AVAILABILITY

The code and implementation details supporting this study are publicly available on GitHub: https://github.com/Hamroz-JONN/Linear-Super-Array

REFERENCES

The source code used to implement the beamformer, evaluate DF and WNG, and generate the results presented in this paper is publicly available at https://github.com/Hamroz-JONN/Linear-Super-Array. The digitized reference values used for quantitative comparison are also provided with the implementation.

Benesty, Jacob, and Jingdong Chen. 2013. *Study and Design of Differential Microphone Arrays*. Vol. 6. Springer Topics in Signal Processing. Springer. https://doi.org/10.1007/978-3-642-33753-6.

Benesty, Jacob, Jingdong Chen, and Chao Pan. 2016. *Fundamentals of Differential Beamforming*. Springer. https://doi.org/10.1007/978-981-10-1046-0.

Chen, Jingdong, Jacob Benesty, and Chao Pan. 2014. "On the Design and Implementation of Linear Differential Microphone Arrays." *The Journal of the Acoustical Society of America* 136 (6): 3097–113. https://doi.org/10.1121/1.4898429.

Chen, Xudong, Jacob Benesty, Gongping Huang, and Jingdong Chen. 2021. "On the Robustness of the Superdirective Beamformer." *IEEE/ACM Transactions on Audio, Speech, and Language Processing* 29: 838–49. https://doi.org/10.1109/TASLP.2021.3050525.

Cox, Henry, Robert M. Zeskind, and Mark M. Owen. 1987. "Robust Adaptive Beamforming." *IEEE Transactions on Acoustics, Speech, and Signal Processing* 35 (10): 1365–76. https://doi.org/10.1109/TASSP.1987.1165054.

Doclo, Simon, and Marc Moonen. 2007. "Superdirective Beamforming Robust Against Microphone Mismatch." *IEEE Transactions on Audio, Speech, and Language Processing* 15 (2): 617–31. https://doi.org/10.1109/TASL.2006.881676.

Huang, Gongping, Jingdong Chen, Jacob Benesty, Israel Cohen, and Xudong Zhao. 2020. "Steerable Differential Beamformers with Planar Microphone Arrays." *EURASIP Journal on Audio, Speech, and Music Processing* 2020 (1): 15. https://doi.org/10.1186/s13636-020-00185-1.

Huang, Weilong, and Emanuel A. P. Habets. 2025. "Robust Differential Beamformers for Linear Superarrays with Non-Uniformly Oriented Directional Microphones." *Proceedings of EUSIPCO 2025*. https://eusipco2025.org/wp-content/uploads/pdfs/0000191.pdf.

Jin, Jilu, Jacob Benesty, Gongping Huang, and Jingdong Chen. 2022. "On Differential Beamforming with Nonuniform Linear Microphone Arrays." *IEEE/ACM Transactions on Audio, Speech, and Language Processing* 30: 1840–52. https://doi.org/10.1109/TASLP.2022.3178232.

Zhang, Hao, Jingdong Chen, and Jacob Benesty. 2015. "Study of Nonuniform Linear Differential Microphone Arrays with the Minimum-Norm Filter." *Applied Acoustics* 98: 62–69. https://doi.org/10.1016/j.apacoust.2015.04.018.

Zheng, Pu, and Yongfeng Zhi. 2025. "Robust Differential Microphone Array with Constant Mainlobe Width and Frequency-Invariant Directivity Factor." *Scientific Reports* 15 (1): 6565. https://doi.org/10.1038/s41598-025-90992-3.